Available online at www.sciencedirect.com
ScienceDirect
Proceedings of the Combustion Institute 000 (2020) 1–10
Proceedings of the Combustion Institute
www.elsevier.com/locate/proci

Flame acceleration in a narrow channel with flow compressibility and diverging or converging walls

Mark Short [a,*], Stephen J. Voelkel [a], David A. Kessler [b]

[a] *Los Alamos National Laboratory, Los Alamos, NM 87544, USA*
[b] *Laboratory for Computational Physics and Fluid Dynamics, Naval Research Laboratory, Washington, USA*

Received 7 November 2019; accepted 28 June 2020
Available online xxx

Abstract

We study the effects of non-parallel (diverging or converging) channel walls on flame propagation and acceleration in planar and cylindrical narrow channels, closed at the ignition end and open at the other, accounting for thermal expansion in both the zero Mach number and weakly compressible flow limits. For parallel channel walls, previous work has shown that thermal expansion induces an axial flow in the channel, which can significantly increase the propagation speed and acceleration of the flame. In this study, we consider examples of diverging/converging linear walls, although our asymptotic analysis is also valid for curved walls. The slope of the channel walls is chosen so that the magnitude of the thermal-expansion induced flow through the channel obtained for parallel walls is modified at leading-order, thereby influencing the leading-order flame propagation. For zero Mach number flows, the effect of the diverging/converging channel walls is moderate. However, for weakly compressible flows, the non-parallel walls directly affect the rate at which pressure diffuses through the channel, significantly inhibiting flame acceleration for diverging walls, whereas the flame acceleration process is enhanced for converging walls. We consider several values of the compressibility factor and channel wall slopes. We also show that the effect of a cylindrical channel geometry can act to significantly enhance flame acceleration relative to planar channels. The study reveals several new physical insights on how non-parallel channel walls can influence the ability of flames to accelerate by modifying the flow and pressure distribution induced by thermal expansion.

Keywords: Flame acceleration; Narrow channel; Diverging/converging channel; Compressibility

1. Introduction

The process of flame acceleration is important to a number of combustion applications. In particular, flame acceleration is the primary stage of the deflagration-to-detonation (DDT) event in gases. The physics of the acceleration process are complex [1–6] and only limited theoretical analysis is possible. However, one avenue to study some of the mechanics of the interaction between the combustion-generated flow field and flame acceleration is via the narrow channel limit [7–14], utilizing a small Peclet

* Corresponding author.
E-mail address: short1@lanl.gov (M. Short).

https://doi.org/10.1016/j.proci.2020.06.329
1540-7489

number (Pe) limit based on the ratio of the channel width to laminar flame thickness. The study of flame propagation and acceleration in the $Pe \to 0$ limit is also important to the understanding of the dynamics of microscale combustion [15–17] and the DDT process at such scales [18].

Daou and Matalon [7,8] examined the properties of steady flame propagation in adiabatic and non-adiabatic thin channels, assuming constant density flow. The small Pe asymptotic study of Short and Kessler [9] extended the work of [7,8] to examine the behavior of variable density, steadily propagating flames in a narrow planar or cylindrical geometry utilizing the zero Mach number limit, thereby accounting for the effects of thermal expansion. They constructed a separable solution for the axial momentum equation that describes an amplitude-modulated Poiseuille (Hagan–Poiseuille) flow in the planar channel (cylinder), generated by thermal expansion of the propagating flame and constrained by geometry and wall friction. Amongst other cases, Short and Kessler [9] examined behavior in a channel closed at one end and open at the other, studying both flame propagation away from, and toward, the closed end. Thermal expansion of the combustion gases was shown to have a significant effect on the steady flame propagation dynamics. For instance, in an adiabatic planar channel and for propagation away from the closed end, it was shown that thermal expansion caused a Poiseuille flow to be generated upstream of the flame with an amplitude $3(\tilde{T}_a/\tilde{T}_u - 1)/2$ along the channel centerline, with the flame propagating at a speed $\tilde{s}_f \tilde{T}_a/\tilde{T}_u$, where $\tilde{T}_a$ is the adiabatic flame temperature, $\tilde{T}_u$ the reactant temperature and $\tilde{s}_f$ the adiabatic laminar flame speed. Pearce and Daou [10] subsequently accounted for the effects of a large amplitude inlet Poiseuille flow on steady flame propagation in a narrow channel, assuming an O(1) Pe number based on the ratio of the inlet flow amplitude to laminar flame speed.

The small Pe variable-density flow framework was expanded to arbitrary unsteady flows by Short and Kessler [11], constructing an integral constraint for the axial Poiseuille flow magnitude as a function of the temporal rate-of-change of density in the channel. Kurdyumov and Matalon [12] examined the quasi-steady evolution of flames in a narrow channel of finite length open at both ends, and, accounting for thermal expansion, showed that a flame will accelerate at a nearly constant rate as it moves down the channel. Kagan et al. [13] and Kurdyumov and Matalon [14] then extended the narrow channel problem to account for the effect of weak compressibility by assuming that the characteristic flame Mach number (Ma) is of the same order as the Peclet number, i.e. $Ma = O(Pe)$ with $Pe = o(1)$. Slip effects were not included in these studies. Kagan et al. [13] also derived an evolution equation for the diffusion of pressure in the channel that occurs due to the compressibility effect. In particular, in most cases, compressibility effects are shown to drive the acceleration of the flame to speeds significantly above the adiabatic laminar flame speed [14]. Kurdyumov and Matalon [14] also showed that acceleration away from the closed end of a channel can ultimately limit to a steadily propagating, high-speed flame.

In the present study, we further extend the above asymptotic studies to one which considers the effects of non-parallel (diverging or converging) channel walls on thermal expansion and flame acceleration in a narrow channel. The deflection amplitude of the walls is chosen to generate an order one change in the induced flow through the channel, thereby influencing the leading-order flame propagation. The theory is valid for curved walls, although we only consider results for linear walls in the current study. The study reveals several new physical insights on how non-parallel channel walls can influence the flame acceleration and propagation mechanism.

2. Model

Flow equations for planar/cylindrical channel flow: We assume a one-step reaction, Fuel $\to$ Product, with an ideal gas equation of state. The nondimensional compressible flow equations are

$$\frac{\mathrm{D}\rho}{\mathrm{D}t} + \rho(\nabla\cdot\mathbf{v}) = 0, \quad \rho\frac{\mathrm{D}\mathbf{v}}{\mathrm{D}t} = -\frac{1}{Ma^2}\nabla p + \frac{Pr}{Pe}\nabla\cdot\tau,$$
$$\rho\frac{\mathrm{D}T}{\mathrm{D}t} = \frac{(\gamma-1)}{\gamma}\frac{\mathrm{D}p}{\mathrm{D}t} + \frac{1}{Pe}\nabla^2 T + Q\,Da\,Pe\,\rho^2\omega_F + \frac{(\gamma-1)}{\gamma}Ma^2\frac{Pr}{Pe}(\tau:\nabla\mathbf{v}),$$
$$p = \rho T, \quad \rho\frac{\mathrm{D}Y}{\mathrm{D}t} = \frac{1}{PeLe}\nabla^2 Y - Pe\,Da\,\rho^2\omega_F, \quad (1)$$

for temperature T, fluid velocity $\mathbf{v} = (v, w)$, density ρ, pressure p, fuel mass fraction Y, spatial coordinate $\mathbf{x} = (r, z)$ and time t. The stress tensor and reaction rate are

$$\tau = \nabla\mathbf{v} + (\nabla\mathbf{v})^{\mathrm{T}} - \frac{2}{3}(\nabla\cdot\mathbf{v})\mathbf{I}, \quad \omega_F = Y\exp(-\theta/T). \quad (2)$$

The non-dimensionalization is based on $\rho = \tilde{\rho}/\tilde{\rho}_u$, $p = \tilde{p}/\tilde{p}_u$, $T = \tilde{T}/\tilde{T}_u$, $\mathbf{v} = \tilde{\mathbf{v}}/\tilde{s}_F$, $\mathbf{x} = \tilde{\mathbf{x}}/\tilde{d}$, $t = \tilde{t}/(\tilde{d}/\tilde{s}_F)$, where $\{\tilde{}\}$ represents dimensional quantities, $\{\}_u$ the unreacted state, and $\tilde{T}_u = \tilde{p}_u/[\tilde{\rho}_u(\tilde{R}/\tilde{W})]$. Here $\tilde{s}_F$ is a representative laminar flame speed, while the length scale $\tilde{d}$ is representative of the half-width or radius in a parallel-walled planar channel or cylindrical geometry respectively. The nondimensional groups in (1) are the Peclet number Pe, Prandtl number Pr, Lewis number Le, Mach number Ma, adiabatic gamma γ, reaction enthalpy Q, Damköhler number Da and activation

Please cite this article as: M. Short, S.J. Voelkel and D.A. Kessler, Flame acceleration in a narrow channel with flow compressibility and diverging or converging walls, Proceedings of the Combustion Institute, https://doi.org/10.1016/j.proci.2020.06.329

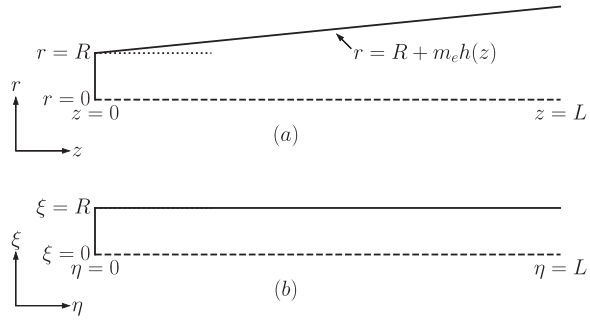

Fig. 1. (a) Planar channel or axisymmetric cylinder geometry (r, z) with linearly diverging walls and a symmetry line along $r = 0$. (b) The transformation (4) maps the upper half of (a) into a rectangular domain in (ξ, η) space.

energy θ, where

$$Pe = \frac{\tilde{\rho}_u \tilde{s}_F \tilde{d} \tilde{c}_p}{\tilde{\lambda}_g},\ Pr = \frac{\tilde{\mu}\tilde{c}_p}{\tilde{\lambda}_g},\ Le = \frac{\tilde{\lambda}_g}{\tilde{c}_p \tilde{\rho} \tilde{D}},$$
$$Ma = \frac{\tilde{s}_F^2}{\tilde{p}_u/\tilde{\rho}_u},\ \gamma = \frac{\tilde{c}_p}{\tilde{c}_p - \tilde{R}/\tilde{W}},\ Q = \frac{\tilde{Q}}{\tilde{c}_p \tilde{T}_u},$$
$$Da = \frac{\tilde{k}\tilde{\lambda}_g}{\tilde{\rho}_u^2 \tilde{c}_p \tilde{s}_F^2},\ \theta = \frac{\tilde{E}}{\tilde{R}\tilde{T}_u}. \tag{3}$$

Here $\tilde{\mu}$, $\tilde{c}_p$, $\tilde{R}$, $\tilde{W}$, $\tilde{\lambda}_g$ $\tilde{Q}$, $\tilde{k}$ and $\tilde{E}$ are the shear viscosity, specific heat, universal gas constant, gas mixture mean molecular weight, thermal conductivity, specific reaction enthalpy of the fuel species, rate constant and activation energy. For the purposes of the present study, these quantities are taken to be constant. Also, $\tilde{D}$ is the fuel mass diffusivity, where the ratio $\tilde{\rho}\tilde{D}$ is constant.

Geometry and Re-Mapping: We consider a symmetric two-dimensional planar channel or axisymmetric cylinder in a coordinate system (r, z), in which the upper and lower walls are specified by some shape $r = \pm[R + m_e h(z)]$ respectively (see Fig. 1a), with $h(0) = 0$ and $h'(z) = O(1) > 0$. Thus m_e is a parameter whose magnitude is representative of the spatial gradient of the wall shape, with $m_e > 0$ representing a diverging channel as in Fig. 1a, and $m_e < 0$ representing a converging channel. The channel region extends axially for $0 \le z \le L$, and is closed at the left end and open at the right. Without loss of generality for the thin channel limit considered below, the flow is assumed symmetric about $r = 0$. Then, the boundary conditions along the upper wall $r = R + m_e h(z)$, assuming the wall is adiabatic, are $\mathbf{n} \cdot \nabla T = 0$, $\mathbf{n} \cdot \nabla Y = 0$, and $\mathbf{v} = \mathbf{0}$, while along $r = 0$, $\partial T/\partial r = 0$, $\partial Y/\partial r = 0$, $\partial p/\partial r = 0$, $v = 0$, and $\partial w/\partial r = 0$.

For asymptotic analysis purposes, it is convenient to transform the upper half of the domain in Fig. 1a to a rectangular one defined by $0 \le \xi \le R$, $0 \le \eta \le L$ (Fig. 1b). The mapping (r, z) to (ξ, η) is defined by

$$r = \left(1 + R^{-1} m_e h(\eta)\right)\xi, \quad z = \eta, \quad t = \tau, \tag{4}$$

where

$$\frac{\partial}{\partial r} = \frac{1}{\left(1 + \hat{m}_e \hat{h}(\hat{\eta})/R\right)} \frac{\partial}{\partial \xi},$$
$$\frac{\partial}{\partial z} = \frac{\partial}{\partial \eta} - \frac{m_e h'(\eta)\xi}{R\left(1 + \hat{m}_e \hat{h}(\hat{\eta})/R\right)} \frac{\partial}{\partial \xi}, \tag{5}$$

from which the required higher derivatives in (1) follow. Boundary conditions along the wall $\xi = R$ become

$$\frac{\partial T}{\partial \xi} = 0,\ \frac{\partial Y}{\partial \xi} = 0,\ v = 0,\ w = 0, \tag{6}$$

and along the symmetry line $\xi = 0$,

$$\frac{\partial T}{\partial \xi} = 0,\ \frac{\partial Y}{\partial \xi} = 0,\ \frac{\partial p}{\partial \xi} = 0,\ v = 0,\ \frac{\partial w}{\partial \xi} = 0. \tag{7}$$

Conditions on the channel flow at the closed and open end boundaries $\eta = 0$ and $\eta = L$ are discussed below.

3. Small Peclet number analysis

Scaling: We now invoke the narrow channel limit $Pe \to 0$ [7–12], rescaling η and τ such that

$$\hat{\eta} = Pe\,\eta,\ \hat{\tau} = Pe\,\tau. \tag{8}$$

The scale of the channel wall deflection should be chosen so that the rate of change in the height of the channel generates an order one change in the induced flow mass flux through the channel, thereby influencing the leading-order flame propagation. As noted above, our analysis considers wall shapes where $h'(\eta) = O(1)$. In order to induce the required mass flux change, a dominant balance argument then requires $m_e h(\eta) = O(1)$, necessitating the additional scalings in light of (8),

$$\hat{m}_e = Pe^{-1} m_e, \quad \hat{h}(\hat{\eta}) = Pe\, h(\eta), \tag{9}$$

so that $m_e h(\eta) = \hat{m}_e \hat{h}(\hat{\eta}) = O(1)$. Finally, as in [13,14], we consider the weakly compressible flow limit $Ma \to 0$, with $Ma = O(Pe)$, i.e.

$$a\,Pe = Ma, \tag{10}$$

Please cite this article as: M. Short, S.J. Voelkel and D.A. Kessler, Flame acceleration in a narrow channel with flow compressibility and diverging or converging walls, Proceedings of the Combustion Institute, https://doi.org/10.1016/j.proci.2020.06.329

with $a = O(1)$. When $a \to 0$, the zero Mach number limit [9,11] is recovered. As in [13,14], we do not consider wall slip effects for $a = O(1)$ in the current study.

Analysis: With (8)–(10), consideration of the leading-order radial momentum, thermal and rate equations in (1) lead to the orderings,

$$\frac{\partial p}{\partial \xi} \sim O(Pe^2), \quad \frac{\partial^2 T}{\partial \xi^2} \sim O(Pe^2), \quad \frac{\partial^2 Y}{\partial \xi^2} \sim O(Pe^2), \tag{11}$$

from which $p \sim p_0(\hat{\eta}, \hat{\tau})$, $T \sim T_0(\hat{\eta}, \hat{\tau})$ and $Y \sim Y_0(\hat{\eta}, \hat{\tau})$ after using the symmetry conditions (7) along $\xi = 0$ for T_0 and Y_0. Based on [9,11], we now seek expansions

$$\begin{aligned} &T \sim T_0(\hat{\eta}, \hat{\tau}) + Pe^2 T_1(\xi, \hat{\eta}, \hat{\tau}), \ p \sim p_0(\hat{\eta}, \hat{\tau}), \\ &Y \sim Y_0(\hat{\eta}, \hat{\tau}) + Pe^2 Y_1(\xi, \hat{\eta}, \hat{\tau}), \ \rho \sim \rho_0(\hat{\eta}, \hat{\tau}), \\ &v \sim Pe\, v_0(\xi, \hat{\eta}, \hat{\tau}), \ w \sim w_0(\xi, \hat{\eta}, \hat{\tau}). \end{aligned} \tag{12}$$

The leading-order axial momentum equation leads to a separable solution for w_0, where, after using (6) and (7),

$$w_0 = \bar{w}_0(\hat{\eta}, \hat{\tau})(R^2 - \xi^2), \tag{13}$$

corresponding to an amplitude-modulated Poiseuille (planar channel) or Hagan–Poiseuille (cylindrical) flow, but now relative to the transformed coordinate ξ, and where

$$\bar{w}_0 = -\frac{1}{2a^2 \sigma Pr}\left(1 + \frac{\hat{m}_e}{R}\hat{h}(\hat{\eta})\right)^2 \frac{\partial p_0}{\partial \hat{\eta}}, \tag{14}$$

with $\sigma = 1$ for planar and $\sigma = 2$ for cylindrical geometries. Eq. (14) relates $\bar{w}_0$ to the pressure gradient in the channel for $a = O(1)$. It shows that for a given pressure gradient, the axial speed amplitude depends on the wall shape, and this will affect the amount of gas that the flame can push through the channel. For the zero Mach number limit $a \to 0$, $p_0 \sim 1 + a^2 p_1$, and a different form from (14) must be used to determine $\bar{w}_0$.

The $O(Pe^2)$ thermal equation, when integrated with ξ between $\xi = 0$ and $\xi = R$ and applying (6) and (7), gives

$$\begin{aligned} &\frac{p_0}{T_0}\frac{\partial T_0}{\partial \hat{\tau}} + \frac{(5-\sigma)}{6}\frac{p_0}{T_0}\bar{w}_0 R^2 \frac{\partial T_0}{\partial \hat{\eta}} \\ &= \frac{(\gamma - 1)}{\gamma}\frac{\partial p_0}{\partial \hat{\tau}} + \frac{\partial^2 T_0}{\partial \hat{\eta}^2} + QDa\frac{p_0^2}{T_0^2}\omega_{F0}. \end{aligned} \tag{15}$$

Note that the energy dissipation terms in (1) cancel with the advection component of pressure [13,14] even for non-parallel walls and/or cylindrical geometries. For $a \to 0$, $p_0 = 1$ and $\partial p_0/\partial \hat{\tau} = 0$ and the channel shape only affects the advection of T_0 through the change in $\bar{w}_0$. Similarly, the leading-order rate equation, integrated between $\xi = 0$ and $\xi = R$ and using (6) and (7), gives

$$\begin{aligned} &\frac{p_0}{T_0}\frac{\partial Y_0}{\partial \hat{\tau}} + \frac{(5-\sigma)}{6}\frac{p_0}{T_0}\bar{w}_0 R^2 \frac{\partial Y_0}{\partial \hat{\eta}} \\ &= \frac{1}{Le}\frac{\partial^2 Y_0}{\partial \hat{\eta}^2} - Da\frac{p_0^2}{T_0^2}\omega_{F0}, \end{aligned} \tag{16}$$

where for $a \to 0$, the channel shape again only affects the advection of Y_0 through the change in $\bar{w}_0$.

The mass equation at $O(Pe)$ leads to an expression for the radial flow component, $v_0(\xi, \hat{\eta}, \hat{\tau})$. When integrated with ξ, applying $v_0 = 0$ on $\xi = 0$ and $\xi = R$, and using (15), the distribution of $\bar{w}_0$ with $\hat{\eta}$ through the channel is derived in differential form as

$$\begin{aligned} &\frac{\partial \bar{w}_0}{\partial \hat{\eta}} + \frac{(\sigma+2)\bar{w}_0}{2\left(1 + \hat{m}_e\hat{h}(\hat{\eta})/R\right)^{\sigma} p_0} \\ &\times \left[T_0 \frac{\partial}{\partial \hat{\eta}}\left\{\frac{2\left(1 + \hat{m}_e\hat{h}(\hat{\eta})/R\right)^{\sigma} p_0}{(\sigma+2)T_0}\right\}\right. \\ &\left. + \frac{(5-\sigma)p_0}{6T_0}\left(1 + \frac{\hat{m}_e}{R}\hat{h}(\hat{\eta})\right)^{\sigma}\frac{\partial T_0}{\partial \hat{\eta}}\right] \\ &= \frac{(\sigma+2)}{2p_0 R^2}\left[-\frac{1}{\gamma}\frac{\partial p_0}{\partial \hat{\tau}} + \frac{\partial^2 T_0}{\partial \hat{\eta}^2} + QDa\frac{p_0^2}{T_0^2}\omega_{F0}\right]. \end{aligned} \tag{17}$$

This form for $\bar{w}_0$ is valid for $a \to 0$, where $p_0 = 1$ and $\partial p_0/\partial \hat{\tau} = 0$, and also is equivalent to (14) for $a = O(1)$. Also, for $a = O(1)$, (14), (15) and (17) can be combined with the equation of state $p_0 = \rho_0 T_0$ to yield an evolution equation for pressure [13],

$$\begin{aligned} &\frac{1}{\gamma}\frac{\partial p_0}{\partial \hat{\tau}} = \frac{R^2}{a^2[(1+\sigma)^2 - 1]Pr} \\ &\times \left\{\frac{\partial}{\partial \hat{\eta}}\left[\left(1 + \frac{\hat{m}_e}{R}\hat{h}(\hat{\eta})\right)^2 p_0 \frac{\partial p_0}{\partial \hat{\eta}}\right]\right. \\ &\left. + \frac{\sigma}{2}\frac{\partial}{\partial \hat{\eta}}\left[\left(1 + \frac{\hat{m}_e}{R}\hat{h}(\hat{\eta})\right)^2\right] p_0 \frac{\partial p_0}{\partial \hat{\eta}}\right\} \\ &+ \frac{\partial^2 T_0}{\partial \hat{\eta}^2} + QDa\frac{p_0^2}{T_0^2}\omega_{F0}. \end{aligned} \tag{18}$$

This equation describes the diffusion, dissipation and transport of pressure through the channel as a result of the effects of weak compressibility. Non-parallel channel walls appear to have a significant influence, as will become apparent in Section 4, modifying the coefficients of the diffusion and transport terms in (18). Finally, the rate term ω_{F0} is

$$\omega_{F0} = Y_0 \exp(-\theta/T_0). \tag{19}$$

Boundary conditions: On $\hat{\eta} = 0$, we have a closed channel with adiabatic wall conditions for which,

$$\bar{w}_0 = 0, \quad \frac{\partial T_0}{\partial \hat{\eta}} = 0, \quad \frac{\partial Y_0}{\partial \hat{\eta}} = 0. \tag{20}$$

Please cite this article as: M. Short, S.J. Voelkel and D.A. Kessler, Flame acceleration in a narrow channel with flow compressibility and diverging or converging walls, Proceedings of the Combustion Institute, https://doi.org/10.1016/j.proci.2020.06.329

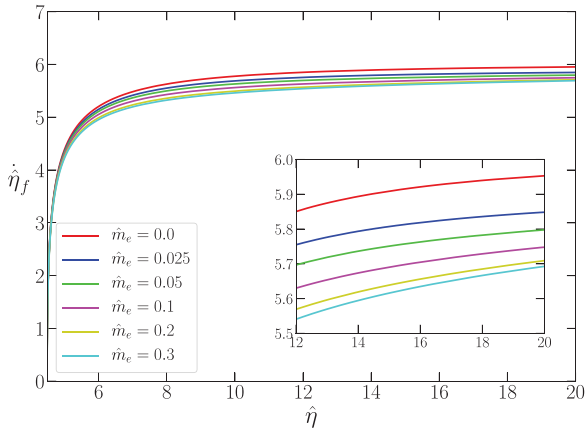

Fig. 2. Flame speed $\dot{\hat{\eta}}_f$ as a function of distance down the channel $\hat{\eta}$ for a planar geometry ($\sigma = 1$) and for $a = 0$ with varying $\hat{m}_e \geq 0$.

For $a = 0(1)$, this implies $\partial p_0/\partial\hat{\eta} = 0$ on $\hat{\eta} = 0$. On $\hat{\eta} = \hat{L}$, $\hat{L} = Pe\,L$, we have an open channel with the constant pressure outflow conditions,

$$p_0 = 1, \quad \frac{\partial T_0}{\partial\hat{\eta}} = 0, \quad \frac{\partial Y_0}{\partial\hat{\eta}} = 0. \tag{21}$$

Channel boundary shape: For this study, we restrict our attention to a linear wall shape, for which $\hat{h}(\hat{\eta}) = \hat{\eta}$. The magnitude of $\hat{m}_e$ then sets the channel wall slope, with $\hat{m}_e > 0$ corresponding to a diverging channel and $\hat{m}_e < 0$ corresponding to a converging channel.

Parameters: We take the base parameters θ, Q, γ, Le consistent with [14], for which $\theta = 72$, $Q = 5$, $\gamma = 1.4$ and $Le = 1$. We also assume $Pr = 1$. The Damköhler number is given by

$$Da = \frac{\theta^2 Q^2}{2Le(1+Q)^2 s_c^2} \exp\left[\frac{\theta}{(1+Q)}\right], \tag{22}$$

where from [14], we set $s_c = 1.0548$. This ensures the adiabatic laminar flame speed is one. The parameters that will be varied below are a, $\hat{m}_e$ and σ.

Numerical solution: For finite a, (14), (15), (16) and (18) are solved for $\bar{w}_0$, p_0, T_0 and Y_0. For $a = 0$, (15), (16) and (17) are solved for T_0, Y_0 and $\bar{w}_0$ with $p_0 = 1$ and $\partial p_0/\partial\hat{\tau} = 0$. In either case, we solve in the positive domain $0 \leq \hat{\eta} \leq \hat{L}$, where, in the following, $\hat{L} = 25$. We also set $R = 1$, i.e the channel width at $\hat{\eta} = 0$ is one. A second-order discretization in space is used on a uniform mesh with spacing $\Delta\hat{\eta} = 0.005$, with a second-order Heun's predictor-corrector method in time. At this resolution, the flame reaction zone structure was well resolved, and all simulations were verified to be grid converged. The flame position, $\hat{\eta} = \hat{\eta}_f(\hat{\tau})$, during the evolution is tracked by the marker $Y_0 = 0.5$, while high-order local differencing is used to obtain the flame speed $\dot{\hat{\eta}}_f(\hat{\tau}) = d\hat{\eta}_f/d\hat{\tau}$ from the trajectory $\hat{\eta}_f(\hat{\tau})$. For initial conditions, the flame is initiated via a hot-spot on $0 \leq \hat{\eta} \leq 4$, where $T_0 = 1 + Q$, $p_0 = 1$ and $\bar{w}_0 = 0$. A linear gradient in T_0 and Y_0 over $4 \leq \hat{\eta} \leq 5$ is used to connect the hot-spot to the initial reactant state, where $T_0 = 1$, $Y_0 = 1$, $p_0 = 1$ and $\bar{w}_0 = 0$. As in [14], we found that the structure and dimension of the hot-spot play a minimal role in the flame acceleration process described in Section 4. Simulations are terminated when $\hat{\eta}_f = 20$.

4. Results

Figure 2 shows the evolution of the flame speed $\dot{\hat{\eta}}_f$ as a function of distance down the channel $\hat{\eta}$ for a planar geometry ($\sigma = 1$) for the zero Mach number limit $a = 0$, comparing a uniform channel ($\hat{m}_e = 0$) with a diverging one for various $\hat{m}_e > 0$. The largest $\hat{m}_e$ considered is 0.3, where the channel expands from $r = 1$ at $\hat{\eta} = 0$ to $r = 8.5$ at $\hat{\eta} = 25$ (Eq. (4)). In sufficiently long channels, for $\hat{m}_e = 0$, a steady flame will develop propagating at the speed $\dot{\hat{\eta}}_f = 1 + Q = 6$ [9], the result of thermal expansion generating an axial flow speed amplitude $\bar{w}_0 = 3Q/2 = 7.5$ ahead of the flame. For the finite length channel $\hat{L} = 25$ with $\hat{m}_e = 0$, the flame accelerates rapidly after the ignition event before slowly evolving toward the limiting speed of 6 (Fig. 2). As $\hat{m}_e$ is increased, the initial transient is similar to that for $\hat{m}_e = 0$, but thereafter the flame accelerates at a progressively slower rate for increasing $\hat{m}_e$. However, for $a = 0$, it is apparent that the wall divergence only weakly affects the flame acceleration. It was noted in Section 2 that for $a = 0$, $\hat{m}_e$ only directly influences $\bar{w}_0$, and thus T_0 and Y_0 are only affected through their advection components in (15) and (16). For $a = 0$, the only channel divergence term that contributes to $\bar{w}_0$ in (17) is given

Please cite this article as: M. Short, S.J. Voelkel and D.A. Kessler, Flame acceleration in a narrow channel with flow compressibility and diverging or converging walls, Proceedings of the Combustion Institute, https://doi.org/10.1016/j.proci.2020.06.329

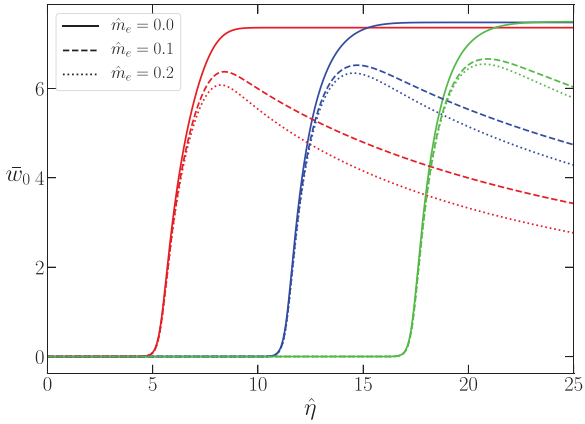

Fig. 3. Spatial variation of $\bar{w}_0$ for $a = 0$ and $\hat{m}_e = 0$, $\hat{m}_e = 0.1$ and $\hat{m}_e = 0.2$ when the flame arrives at $\hat{\eta} = 6$ (red), $\hat{\eta} = 12$ (blue) and $\hat{\eta} = 18$ (green) for each $\hat{m}_e$ case. (For interpretation of the references to color in this figure legend, the reader is referred to the web version of this article.)

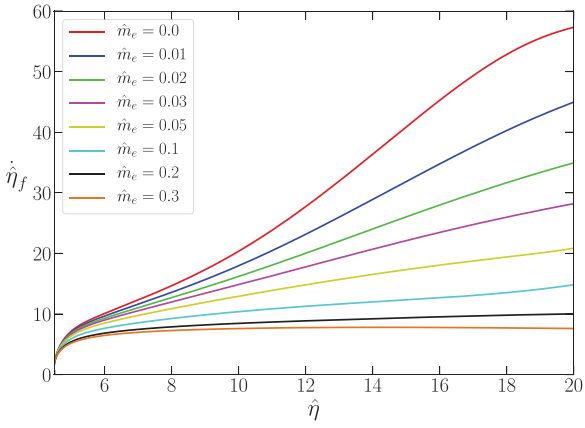

Fig. 4. Flame speed $\dot{\hat{\eta}}_f$ as a function of distance down the channel $\hat{\eta}$ for a planar geometry ($\sigma = 1$) and for $a = 0.25$ with varying $\hat{m}_e \geq 0$.

by $\bar{w}_0 \sigma \hat{m}_e/(1 + \hat{m}_e \hat{\eta})$ for $\hat{h}(\hat{\eta}) = \hat{\eta}$ and $R = 1$. With this in mind, Fig. 3 compares the spatial variation of $\bar{w}_0$ for $\hat{m}_e = 0$, $\hat{m}_e = 0.1$ and $\hat{m}_e = 0.2$ when the flames arrive at various fixed locations in channel. Locally within the flame structures, even for $\hat{m}_e > 0$, there is a rapid rise in $\bar{w}_0$. The peak $\bar{w}_0$ drops as $\hat{m}_e$ increases. The channel divergence does, however, affect the distribution of $\bar{w}_0$ on a longer spatial scale ahead for the flame, reducing $\bar{w}_0$ with increasing $\hat{\eta}$. Due to the $\bar{w}_0$ structure (Fig. 3), the distributions of T_0 and Y_0 within the flame are also only moderately affected by varying $\hat{m}_e$. This underlies the weak influence of $\hat{m}_e$ seen in Fig. 2 for $a = 0$. We comment in more detail below on the flow effect of converging channels ($m_e < 0$), but we remark at this point that channel convergence has a similarly weak effect on the flame acceleration process for $a = 0$.

Consideration of a non-zero compressibility factor a leads to a much stronger influence of m_e. We know from [13,14] that, for $\hat{m}_e = 0$ and non-zero a, compressibility driven pressure diffusion in the channel (determined by (18)) is responsible for driving a rapid flame acceleration in a finite length channel closed at the ignition end, to speeds that are many tens larger than the laminar flame speed. Figure 4 shows the evolution of the flame speed $\dot{\hat{\eta}}_f$ as a function of $\hat{\eta}$ for a planar channel geometry ($\sigma = 1$) with varying $\hat{m}_e \geq 0$ for $a = 0.25$. For $\hat{m}_e = 0$, we observe a very rapid flame acceleration consistent with [14]. However, for only small increases in $\hat{m}_e$ in the range $0 < \hat{m}_e \leq 0.03$, the rapid flame acceleration observed for $\hat{m}_e = 0$ is significantly hindered and the flame attains progressively lower speeds in the channel. For $\hat{m}_e > 0.03$, the rate of retardation of the flame acceleration begins to slow as the flame speed attained in the channel drops. For sufficiently large $\hat{m}_e$, it appears that the flame speed approaches $\dot{\hat{\eta}}_f = 6$, i.e. the limiting speed without compressibility.

Please cite this article as: M. Short, S.J. Voelkel and D.A. Kessler, Flame acceleration in a narrow channel with flow compressibility and diverging or converging walls, Proceedings of the Combustion Institute, https://doi.org/10.1016/j.proci.2020.06.329

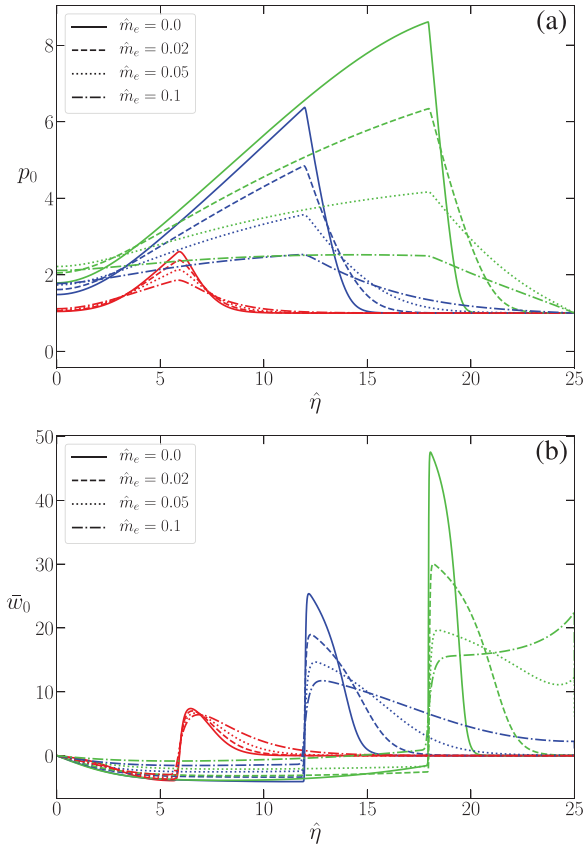

Fig. 5. (a) Spatial variation of p_0 for $a = 0.25$ and $\hat{m}_e = 0$, $\hat{m}_e = 0.02$, $\hat{m}_e = 0.05$ and $\hat{m}_e = 0.1$ when the flame arrives at $\hat{\eta} = 6$ (red), $\hat{\eta} = 12$ (blue) and $\hat{\eta} = 18$ (green). (b) As for (a), but for $\bar{w}_0$. (For interpretation of the references to color in this figure legend, the reader is referred to the web version of this article.)

This behavior can be explained by considering the evolution of p_0 and $\bar{w}_0$ in the channel for different $\hat{m}_e$ as shown in Fig. 5. The right-hand-side of Eq. (18) shows how the coefficients of the pressure diffusion and transport terms are modified by the diverging channel walls. In particular, $\hat{m}_e > 0$ causes the pressure diffusion coefficients to increase in magnitude, and thus pressure diffuses more rapidly as $\hat{m}_e$ increases. Figure 5a,b show that it is precisely this effect which retards the flame acceleration process. For $\hat{m}_e = 0$, there is a large pressure build-up in the channel through the effects of (18), along with a sharp increase in $\bar{w}_0$ locally within the flame. Ahead of the flame, both p_0 and $\bar{w}_0$ drop rapidly. For $\hat{m}_e > 0$, pressure diffuses more rapidly, and the peak pressure p_0 and axial speed $\bar{w}_0$ attained within the flame drop. The p_0 and $\bar{w}_0$ regions become progressively more diffuse ahead of the flame. As $\hat{m}_e$ continues to increase, this effect is amplified, and for $\hat{m}_e$ large enough, pressure diffusion is so rapid that there is no significant pressure build up in the channel and the flame speed approaches $\hat{\dot{\eta}}_f = 6$.

Figure 6 shows the evolution of $\hat{\dot{\eta}}_f$ as a function of $\hat{\eta}$ for $\sigma = 1$ with varying $m_e \geq 0$ for $a = 1$. For increasing a, the flame acceleration process becomes significantly more rapid. For $\hat{m}_e = 0$, we observe a rapid rise in flame speed giving way to a steadily propagating high-speed flame solution, again driven by the consequences of compressibility-driven pressure diffusion. For $m_e > 0$, the flame acceleration is again retarded. However, as the pressure diffusion effects are more localized around the flame for $a = 1$, larger values of $\hat{m}_e$ are required to cause comparable drops in the flame speed relative to that for $a = 0.25$. For all $m_e > 0$, the flame speed reaches a peak, before weakly decelerating as the flame moves down the channel. The basic mechanism played by pressure diffusion and the generation of axial flow are similar in nature to those of Fig. 5, but with spatial scales that are narrower for $a = 1$ compared to $a = 0.25$.

Consideration of cylindrical geometries also has a significant effect on the flame acceleration process relative to that for a planar channel. Note that

Please cite this article as: M. Short, S.J. Voelkel and D.A. Kessler, Flame acceleration in a narrow channel with flow compressibility and diverging or converging walls, Proceedings of the Combustion Institute, https://doi.org/10.1016/j.proci.2020.06.329

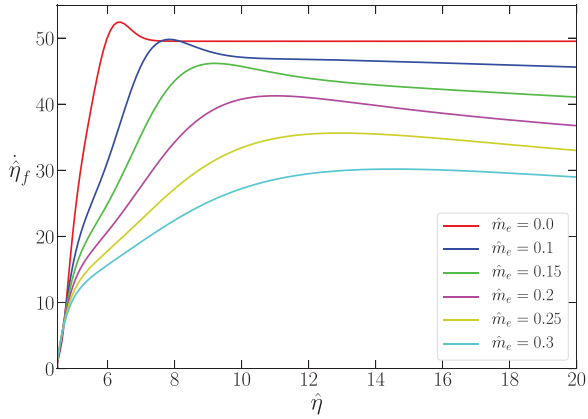

Fig. 6. Flame speed $\hat{\dot{\eta}}_f$ as a function of $\hat{\eta}$ for a planar geometry ($\sigma = 1$) and for $a = 1$ with varying $\hat{m}_e \geq 0$.

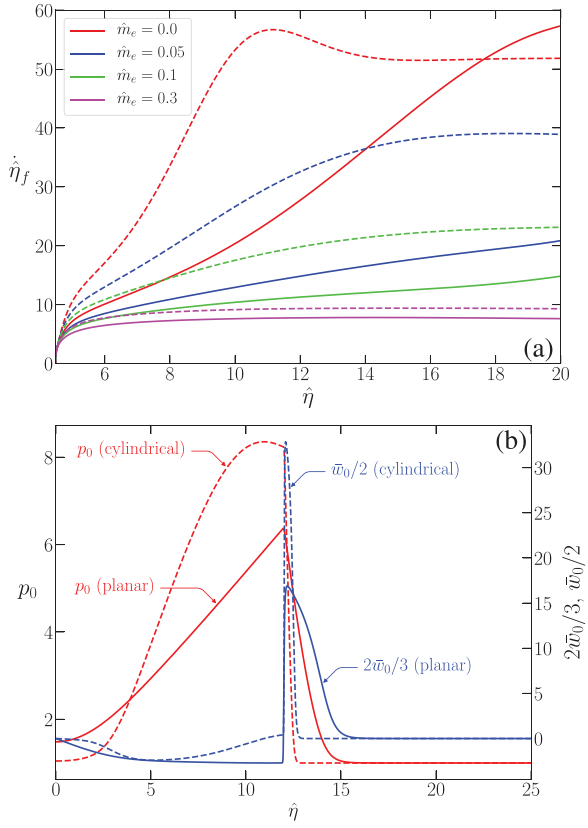

Fig. 7. (a) Flame speed $\hat{\dot{\eta}}_f$ as a function of $\hat{\eta}$ for a cylindrical geometry ($\sigma = 2$) and for $a = 0.25$ with varying $\hat{m}_e \geq 0$ (dashed lines), along with the equivalent ($\sigma = 1$) planar geometry results (solid lines). (b) Spatial variation of p_0 and average axial flow speed $2\bar{w}_0/3$ (planar) or $\bar{w}_0/2$ (cylinder) for $\hat{m}_e = 0$ when the flame arrives at $\hat{\eta} = 12$.

for any a or $\hat{m}_e$, the average axial flow speed for $\sigma = 1$ is $(\int_{-R}^{R} w_0 d\xi)/2R = 2\bar{w}_0/3$, while for $\sigma = 2$, it is $(\int_{-R}^{R} 2\pi\xi w_0 d\xi)/\pi R^2 = \bar{w}_0/2$. For $a = 0$ and $m_e = 0$, σ can be scaled out of (17) by dividing $\bar{w}_0$ by $(\sigma + 2)/2$, so that at any $\hat{\eta}$, $\bar{w}_0$ in the cylindrical geometry is 4/3 larger than for $\sigma = 1$, and thus the average speeds for $\sigma = 1$ and 2 are identical. The convection terms in (15) and (16) are now identical for $\sigma = 1$ and 2, so that geometry does not affect

Please cite this article as: M. Short, S.J. Voelkel and D.A. Kessler, Flame acceleration in a narrow channel with flow compressibility and diverging or converging walls, Proceedings of the Combustion Institute, https://doi.org/10.1016/j.proci.2020.06.329

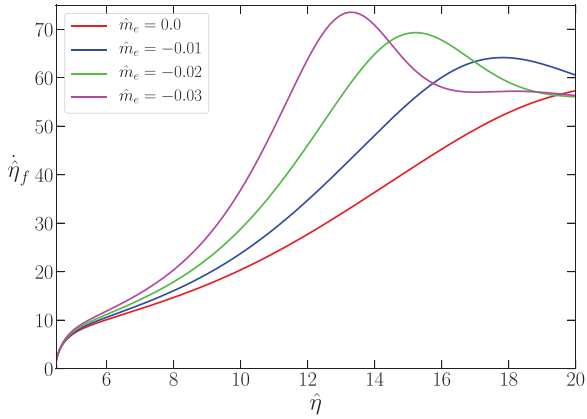

Fig. 8. Flame speed $\dot{\hat{\eta}}_f$ as a function of $\hat{\eta}$ for a planar geometry ($\sigma = 1$) and for $a = 0.25$ with varying $\hat{m}_e \leq 0$.

the propagation rate. However, for $a = 0$ and any $m_e > 0$, σ enters into the flow speed Eq. (17) in a non-trivial way, reducing the average flow speed at any $\hat{\eta}$ in the cylinder below that of the planar channel, leading to the flame accelerating more slowly in the cylinder. For $a > 0$, the dynamics become even become complex, as σ now also affects the diffusion of pressure (18). Figure 7a shows the evolution of $\dot{\hat{\eta}}_f$ with $\hat{\eta}$ for $\sigma = 2$ with varying $\hat{m}_e \geq 0$ and $a = 0.25$, compared with the equivalent evolutions for $\sigma = 1$. For $m_e = 0$, the flame accelerates significantly more rapidly for $\sigma = 2$ than for $\sigma = 1$. During the acceleration, the average axial flow speed and pressure within the flame are larger for $\sigma = 2$, while the pressure diffusion scales are much shorter (Fig. 7b). As m_e increases, the pressure diffusion scales are broadened, and an increasingly smaller difference is found between the $\sigma = 1$ and 2 flame acceleration profiles (Fig. 7a).

The final case we comment on is the effect of a converging channel. Figure 8 shows the evolution of $\dot{\hat{\eta}}_f$ with $\hat{\eta}$ for $\sigma = 1$ with varying $m_e \leq 0$ for $a = 0.25$. The effect of a converging channel on the pressure diffusion Eq. (18) is the reverse to that for $m_e > 0$. In particular, now the pressure diffusion coefficients are lowered for $m_e < 0$, and thus pressure diffuses less rapidly. For $m_e < 0$ we observe a rapid local rise in $\bar{w}_0$ around the flame, becoming more intense as $m_e < 0$ decreases. The pressure rise through the flame is larger, and the pressure drop-off ahead of the flame more rapid. This reverse effect underlies the enhancement of the flame acceleration process seen in Fig. 8. Note that since $r = 1$ at $\hat{\eta} = 0$, a consequence of setting $R = 1$, we must ensure $|m_e|$ is small enough for $r > 0$ at $\hat{\eta} = 25$. Thus for $m_e = -0.03$, we have $r = 0.25$ (Eq. (4)). However, we note that R can be scaled out of (14), (15), (16) and (18) by setting $m_e^* = \hat{m}_e/R$, $w_0^* = R^2\bar{w}_0$ and $a^* = a/R$. Consequently, for example for $\hat{m}_e = -0.03$, the flame evolution seen in Fig. 8 would be similarly obtained for $r = 4$ at $\hat{\eta} = 0$, $\hat{m}_e = -0.12$ (whereby $r = 1$ at $\hat{\eta} = 25$) and also $a = 1$. In short, by decreasing the pressure diffusion coefficients in (18), and thereby supporting the localized growth of p_0 and $\bar{w}_0$ around the flame, a converging channel enhances the flame acceleration process over that observed for $\hat{m}_e = 0$.

5. Summary

We have analyzed the effects of linearly diverging or converging walls with gradient $\hat{m}_e$ on flame propagation and acceleration in planar ($\sigma = 1$) and cylindrical ($\sigma = 2$) narrow channels ($Pe \to 0$), closed at the ignition end, accounting for thermal expansion in the zero Mach number ($Ma = 0$) and weakly compressible flow ($a = Ma/Pe = O(1)$) limits. For zero Mach number flows, the effect of the diverging/converging channel walls is moderate. For $\sigma = 1$, increasingly divergent walls lowers the flame acceleration rate, as the average flow speed of gas pushed through the channel drops. For $a = O(1)$, non-parallel walls modify the rate at which pressure diffuses through the channel, significantly modifying the flame acceleration mechanics seen for $\hat{m}_e = 0$. For increasing $\hat{m}_e > 0$, the pressure diffusion scale lengthens ahead of the flame, causing the flame to accelerate less rapidly. For $\hat{m}_e > 0$ and large enough, pressure diffusion is sufficiently rapid that there is no significant pressure build up in the channel and the flame dynamics are similar to that for $a = 0$. As a increases, the spatial scales for pressure diffusion are shortened, so that larger $\hat{m}_e > 0$ are required to reduce the flame acceleration magnitudes to those for smaller a. Flames accelerate faster in cylindrical geometries than planar ones for fixed $a > 0$ and $\hat{m}_e > 0$ as the average flow rate is increased due to the shorter pressure diffusion scales. Converging channels cause the opposite effect. As $\hat{m}_e < 0$ decreases, the flame accelerates increasingly

Please cite this article as: M. Short, S.J. Voelkel and D.A. Kessler, Flame acceleration in a narrow channel with flow compressibility and diverging or converging walls, Proceedings of the Combustion Institute, https://doi.org/10.1016/j.proci.2020.06.329

more rapidly, caused by an increasing average flow speed and pressure rise through the flame due to the shortening pressure diffusion scale ahead of the flame. In future studies, we will consider the effect of curved walls, heat loss and the potential influence of wall slip on the pressure diffusion process for $a = O(1)$.

Declaration of Competing Interest

The authors declare that they have no known competing financial interests or personal relationships that could have appeared to influence the work reported in this paper.

References

[1] J. Shepherd, J. Lee, in: Major Research Topics in Combustion, Springer, 1992, pp. 439–487.
[2] S. Ciccarelli, S. Dorofeev, *Prog. Eng. Sci.* 34 (2008) 499–550.
[3] K. Dobrego, I. Kozlov, V. Vasiliev, *Int. J. Heat Mass Trans.* 49 (2006) 198–206.
[4] D. Kessler, V. Gamezo, E. Oran, *Combust. Flame* 157 (2010) 2063–2077.
[5] M. Kuznetsov, J. Grune, *Int. J. Hydr. Energy* 44 (2019) 8727–8742.
[6] V. Bychkov, V. Akkerman, G. Fru, A. Petchenko, L. Eriksson, *Combust. Flame* 150 (2007) 263–276.
[7] J. Daou, M. Matalon, *Combust. Flame* 124 (2001) 337–349.
[8] J. Daou, M. Matalon, *Combust. Flame* 128 (2002) 321–329.
[9] M. Short, D. Kessler, *J. Fluid Mech.* 638 (2009) 305–337.
[10] P. Pearce, J. Daou, *J. Fluid Mech.* 754 (2014) 161–183.
[11] M. Short, D. Kessler, in: Proceedings of the 23rd ICDERS, 2011. http://www.icders.org.
[12] V. Kurdyumov, M. Matalon, *Proc. Combust. Inst.* 34 (2013) 865–872.
[13] L. Kagan, P. Gordon, G. Sivashinsky, *Proc. Combust. Inst.* 35 (2015) 913–920.
[14] V. Kurdyumov, M. Matalon, *Combust. Theory Modell.* 34 (2016) 1046–1067.
[15] P. Ronney, *Combust. Flame* 135 (2003) 421–439.
[16] K. Maruta, *Proc. Combust. Inst.* 33 (2011) 125–150.
[17] D. Kessler, M. Short, *Combust. Theory Modell.* 12 (2008) 809–829.
[18] M.-H. Wu, M. Burke, S. Son, R. Yetter, *Proc. Combust. Inst.* 31 (2007) 2429–2436.

Please cite this article as: M. Short, S.J. Voelkel and D.A. Kessler, Flame acceleration in a narrow channel with flow compressibility and diverging or converging walls, Proceedings of the Combustion Institute, https://doi.org/10.1016/j.proci.2020.06.329